Thermo-resistance of ESKAPE-panel pathogens, eradication and growth prevention of an infectious biofilm by photothermal, polydopamine-nanoparticles in vitro

Gao, Ruifang; van der Mei, Henny C; Ren, Yijin; Chen, Hong; Chen, Gaojian; Busscher, Henk J; Peterson, Brandon W

Published in:
Nanomedicine-Nanotechnology biology and medicine

DOI:
10.1016/j.nano.2020.102324

Document Version
Publisher's PDF, also known as Version of record

Publication date:
2021

ELSEVIER

Nanomedicine: Nanotechnology, Biology, and Medicine
32 (2021) 102324

nanomedicine
Nanotechnology, Biology, and Medicine

nanomedjournal.com

Thermo-resistance of ESKAPE-panel pathogens, eradication and growth prevention of an infectious biofilm by photothermal, polydopamine-nanoparticles *in vitro*

Ruifang Gao, MS[a,b], Henny C. van der Mei, PhD[b], Yijin Ren, PhD[c], Hong Chen, PhD[a,*], Gaojian Chen, PhD[a], Henk J. Busscher, PhD[b], Brandon W. Peterson, PhD[b,*]

[a]*College of Chemistry, Chemical Engineering and Materials Science, Soochow University, Suzhou, China*
[b]*University of Groningen, University Medical Center Groningen, Department of Biomedical Engineering, Groningen, The Netherlands*
[c]*University of Groningen, University Medical Center Groningen, Department of Orthodontics, Groningen, The Netherlands*

Revised 4 September 2020

Abstract

Nanotechnology offers many novel infection-control strategies that may help prevent and treat antimicrobial-resistant bacterial infections. Here, we synthesized polydopamine, photothermal-nanoparticles (PDA-NPs) without further surface-functionalization to evaluate their potential with respect to biofilm-control. Most ESKAPE-panel pathogens in suspension with photothermal-nanoparticles showed three- to four-log-unit reductions upon Near-Infra-Red (NIR)-irradiation, but for enterococci only less than two-log unit reduction was observed. Exposure of existing *Staphylococcus aureus* biofilms to photothermal-nanoparticles followed by NIR-irradiation did not significantly kill biofilm-inhabitants. This indicates that the biofilm mode of growth poses a barrier to penetration of photothermal-nanoparticles, yielding dissipation of heat to the biofilm-surrounding rather than in its interior. Staphylococcal biofilm-growth in the presence of photothermal-nanoparticles could be significantly prevented after NIR-irradiation because PDA-NPs were incorporated in the biofilm and heat dissipated inside it. Thus, unmodified photothermal nanoparticles have potential for prophylactic infection-control, but data also constitute a warning for possible development of thermo-resistance in infectious pathogens.

Key words: photothermal nanoparticles; heat conversion; polydopamine; biofilms; *S. aureus*; thermo-resistance

Biofilms are increasingly recognized as an important factor in many chronic, localized bacterial infections.[1] With the threat of infection by antimicrobial-resistant bacterial strains becoming the number one cause of death by the year 2050,[2] new infection-control strategies are needed. Infection-control strategies are either geared towards eradicating an infectious biofilm,[3] when a patient presents sick at the emergency ward of a hospital ("infection therapy"), or towards preventing development of an infectious biofilm after invasive surgery or trauma ("infection prophylaxis").[4] Nanotechnology offers many novel infection-control strategies, amongst which are metal-based nanocomposites,[5] carbon-based nanomaterials[6] and polymer-based nanoparticles.[7] Nanoparticles are attractive for eradication of an existing infectious biofilm, because their small size makes penetration in a biofilm relatively easy.

Photothermal nanoparticles such as gold nano-crosses, gold nano-rods,[8] carbon nanoparticles,[9] metal-organic hybrid structures[10] and different conjugated polymers[11,12] have been

Abbreviations: CCK, cell counting kit; CFU, colony forming unit;; CLSM, confocal laser scanning microscopy; DMEM, Dulbecco's modified eagle medium; DMSO, dimethyl sulfoxide; FBS, fetal bovine serum; NIR, near infra-red; PBS, phosphate buffered saline; PDA-NPs, polydopamine nanoparticles; TSB, tryptone soya broth

Declaration of Conflict of Interest

Financial Support

* Corresponding authors at: Department of Biomedical Engineering-FB40, University Medical Center Groningen, 9713, AV, Groningen, The Netherlands.
E-mail addresses: hongch@suda.edu.cn, (H. Chen), b.w.peterson@umcg.nl. (B.W. Peterson).

https://doi.org/10.1016/j.nano.2020.102324

extensively explored in cancer treatment ("photothermal therapy"). Photothermal nanoparticles convert near infra-red (NIR)-light into heat and therewith have the potential of generating high, local temperatures.[13] Heat is indiscriminately damaging to materials depending local heat generation, dissipation and final temperatures reached. On the bacterial level, this can imply lethal damage to cell wall components, (e)DNA and other intra- or extra-cellular material, regardless of the strain involved or its possible antibiotic-resistance.[14,15] To our knowledge, among human clinical pathogens, no thermo-resistant bacteria have ever been described.

Photothermal treatment of bacterial infections[16–19] largely builds on progress made with respect to tumor treatment, where the majority of research is geared towards evaluating surface modified, photothermal nanoparticles.[20] Yet, this leaves several fundamental questions open with respect to the application of photothermal treatment of bacterial infections on its own, i.e. particularly the use of unmodified photothermal nanoparticles. Many evaluations of unmodified photothermal nanoparticles, such as of graphene oxide,[21] indium selenide[22] and iron carbide,[23] demonstrated broad-spectrum, photothermal killing of different bacterial strains in planktonic state, i.e. suspended in a fluid phase. Yet, although it is known that the majority of bacterial infections are due to bacteria in a protective biofilm-mode of growth,[24,25] less studies with unmodified photothermal nanoparticles have been done on infectious biofilms.[26] This is a severe shortcoming for the clinical translation of photothermal therapy for bacterial infection-control.

Polydopamine is frequently used as a base coating for functionalization of nanoparticles,[27] formation of polymer brush coatings[28] and synthesis of antifouling surfaces.[29] Polydopamine nanoparticles (PDA-NPs) have been extensively explored for tumor eradication[30,31] and are easily self-polymerized from dopamine in solution. PDA-NPs possess high photothermal conversion efficiency,[32] good biocompatibility[33,34] and biodegradability.[35,36] Many studies on bacterial infection-control have used surface-modified PDA-NPs. For instance, PDA-NPs equipped with Indocyanine Green as a photosensitizer, produced reactive oxygen species to eradicate *Staphylococcus aureus* biofilms.[37] PDA-NPs modified with thiol-poly (ethylene glycol) and vancomycin appeared stable in the blood circulation and killed planktonic methicillin-resistant *Staphylococcus aureus* upon NIR-irradiation.[38] Although additional antimicrobial surface modifications to PDA-NPs can provide benefits on top of photothermal killing, they often come at the expense of increased cytotoxicity.[30] Moreover, surface modification can present a hurdle for clinical translation, making regulatory approval more difficult and endangering return of investment for interested market parties due to higher costs.

Considering that the development of photothermal nanoparticles for bacterial infection control has largely "skipped" in-depth evaluation of the merits of unmodified PDA-NPs, the aim of this study is to determine the potential of photothermal PDA-NPs without any surface modification with respect to bacterial infection-control. Two modes of clinical infection treatment will be studied using *in vitro* models: eradication of an existing infectious biofilm (the "therapeutic"-mode") or prevention of the development of an infectious biofilm (the "prophylactic"-mode"). First, we will describe the synthesis of photothermal PDA-NPs and measure their photothermal conversion efficiency, after which their killing efficacy towards planktonic ESKAPE-panel pathogens (in suspension) will be evaluated. ESKAPE is an acronym for the names of six pathogens (*Enterococcus faecium*, *Staphylococcus aureus*, *Klebsiella pneumoniae*, *Acinetobacter baumannii*, *Pseudomonas aeruginosa* and Enterobacter spp.) requiring focus in the development of new infection-control strategies because of their ability to escape killing of commonly used antibiotics.[39–42] Next, an existing *S. aureus* biofilm will be exposed to suspensions of PDA-NPs (therapeutic-mode) and upon NIR-irradiation biofilm viability will be assessed. Note that *S. aureus* is a prominent ESKAPE-panel member, causing a wide variety of human infections.[43] Finally, staphylococcal biofilm growth in the absence and presence of PDA-NPs and NIR-irradiation will be evaluated (prophylactic-mode), followed by assessment of biofilm viability.

Methods

Synthesis and characterization of polydopamine-NPs

The synthesis and characterization of polydopamine nanoparticles (PDA-NPs) can be found in the Supplementary Materials.

Photothermal properties of PDA-NPs

Different suspensions (250 μL) of PDA-NPs (0.05–1 mg/mL) in phosphate buffered saline (PBS, 5 mM K_2HPO_4, 5 mM KH_2PO_4, 150 mM NaCl, pH 7.0) were added in a 96 wells-plate and irradiated at 808 nm using a NIR-laser (Thorlabs, USA). After irradiation for different durations up to 20 min under gentle shaking, suspension temperatures were measured with a digital thermometer (MOSEKO, Gauteng, South Africa). Temperatures were measured at different laser power densities of 260, 520, 780, and 1300 mW/cm^2, as established by optically defocusing the laser beam into a parallel beam with controllable diameter. Temperature measurements were done at pH 7.0 and 5.0 (pH adjusted with HCl) to mimic physiological pH conditions and pH conditions in a biofilm, respectively.

In addition, in order to measure heat losses in the system required for the calculation of the photothermal conversion efficiency, PDA-NPs suspensions were photo-activated at a laser power density of 1300 mW/cm^2 for 5 min after which photo-activation was arrested and temperature decreases due to heat loss to the environment monitored as a function of time. The photothermal conversion efficiency of PDA-NPs was calculated as described in previous studies using measured temperatures.[32,44] Neglecting heat uptake by the PDA-NPs, the temperature change of the system upon NIR-irradiation equals

$$\left(m_{H_2O} C_{p,H_2O}\right) \frac{\mathrm{d}T}{\mathrm{d}t} = Q_s + Q_{NPs} - Q_{loss} \quad (1)$$

where m_{H_2O} and $C_{P,\ H_2O}$ are the mass and specific heat of water, respectively. T is the suspension temperature. Q_s is the heat uptake per unit time associated with the light absorbed by the suspension fluid, Q_{NPs} is the photothermal heat generated by the

PDA-NPs per unit time and Q_{loss} represents the heat loss of the system per unit time. Q_{NPs} can be derived from the NIR absorption spectrum according to

$$Q_{NPs} = I\left(1-10^{A_{808\ nm}}\right) \tag{2}$$

where I is the laser power, $A_{808\ nm}$is the absorbance of PDA-NPs at the wavelength of 808 nm and η is the photothermal conversion efficiency. The heat loss can be expressed as

$$Q_{loss} = hAT \tag{3}$$

where h is the heat transfer coefficient, A is the surface area of the system exposed to its surrounding and ΔT is the temperature difference between the system and its surrounding, i.e. $T - T_{env}$, in which T and T_{env} are the suspension and surrounding temperatures, respectively. At equilibrium, in absence of photothermal PDA-NPs but upon NIR-irradiation, combination of Eqs. (1) and (3) yields

$$Q_s = Q_{loss} = hA\,T_{\ max,H_2O} \tag{4}$$

where $\Delta T_{max,\ H_2O}$is the maximal temperature change of water at equilibrium.

Equally, at equilibrium in the presence of PDA-NPs, the Q_s and Q_{NPs} both contribute to the heat input of the system, and combination of Eqs. (1) and (3) yields

$$Q_{NPs} + Q_s = Q_{loss} = hA\,T_{\ max,suspension} \tag{5}$$

where $\Delta T_{max,\ suspension}$ is the temperature change of the PDA-NPs dispersion at equilibrium. Through insertion of Eqs. 2-5 in Eq. 1, the photothermal conversion efficiency can be expressed as

$$\begin{aligned} &= \frac{hA\,T_{\ max,suspension} - hA\,T_{\ max,H_2O}}{I\left(1-10^{-A_{808\ nm}}\right)} \\ &= \frac{hA\left(T_{\ max,suspension} - T_{\ max,H_2O}\right)}{I\left(1-10^{-A_{808\ nm}}\right)} \end{aligned} \tag{6}$$

where $A_{808\ nm}$ follows from UV-Vis absorption spectroscopy, and $\Delta T_{max,\ H_2O}$ and $\Delta T_{max,\ suspension}$ follow from NIR activation in absence and presence of PDA-NPs, respectively. The laser power I amounts 0.5 W. This leaves hA as an unknown. In order to obtain hA, Eq. 1 can be re-written in absence of photo-activation (i.e. after the laser turned off, implying that $Q_{NPs} + Q_s = 0$) during heat loss to the environment, as

$$\frac{\mathrm{d}T}{\mathrm{d}T_{max}\mathrm{d}t} = -\frac{hA\,T}{T_{max}\left(m_{H_2O}C_{p,H_2O}\right)} \tag{7}$$

Solving this differential equation yields

$$t = -\frac{m_{H_2O}C_{p,H_2O}}{hA}\ \ln\frac{T}{T_{max}} \tag{8}$$

where $-\frac{m_{H_2O}C_{p,H_2O}}{hA}$ can be directly calculated from a graph of $\ln\frac{T}{T_{max}}$ versus time for use in Eq. 6, yielding the photothermal conversion efficiency η.

Bacterial culturing and harvesting

ESKAPE-panel pathogens,[41] including *S. aureus* ATCC 12600 were stored in 7% (v/v) DMSO at −80°C. Of each panel strain, a single colony from a blood agar plate was inoculated in 10 mL of Tryptone Soya Broth (TSB) and incubated aerobically at 37°C for 24 h. Bacterial suspension were then transferred into fresh 200 mL of TSB and incubated for 17 h. Bacteria were harvested by centrifugation at 5000 g for 5 min at 10°C and washed twice with PBS. Bacteria were resuspended in 10 mL PBS and sonicated for 3 × 10 s at 30 W (Vibra Cell model 375, Sonics and Materials Inc., USA) while cooling in an ice/water bath to break possible aggregates. Final concentrations of bacterial suspensions were determined using a Bürker-Türk counting chamber.

Photothermal killing of planktonic ESKAPE-panel pathogens by PDA-NPs

To determine the killing efficiency of PDA-NPs on planktonic ESKAPE-panel pathogens, 2.5 μL of a bacterial suspension in PBS (3×10^8 bacteria/mL) was diluted with a PDA-NPs suspension (0.5 mg/mL PDA-NPs) in 96 well-plates (Greiner Bio-One, Austria) to make ratios of PDA-NPs to bacteria of 4.2×10^5 or 2.1×10^5 nanoparticles per bacterium (for details, see Supplementary Materials). The total volume in the wells was 250 μL. Next, the mixed suspensions were irradiated for 10 min with a NIR-laser at a power density of 1300 mW/cm^2. After irradiation, bacterial suspensions were serially diluted and plated on TSB agar plates. After overnight incubation at 37°C, the number of colony-forming units (CFU) was counted. All experiments were carried out with bacteria grown from three separate bacterial cultures.

Photothermal killing of existing S. aureus biofilms by PDA-NPs

Therapeutic use of photothermal nanoparticles implies the eradication of an existing infectious biofilm. To this end, a staphylococcal biofilm was grown on a glass surface (0.4 cm × 0.4 cm × 0.1 cm), cut from a microscope slide (ThermoFisher, Germany). Before biofilm growth, glass surfaces were cleaned with a piranha solution (3:10:3, v:v:v, NH_4OH: ultrapure water: H_2O_2) rinsed with copious amounts of water, followed by rinsing twice with absolute ethanol. Cleaned glass samples were stored in ethanol and dried with filtered nitrogen immediately before use.

Cleaned and dried glass samples were placed in a 96 well-plate and 100 μL of a *S. aureus* ATCC 12600 suspension (1×10^9 bacteria/mL) in PBS was added to the wells and left to sediment for 1 h at 37°C to allow bacteria to adhere. Next, the suspensions were removed, and the wells were washed once with 100 μL of PBS. Subsequently, 200 μL of TSB was added and staphylococci were grown at 37°C for 48 h and after 24 h the TSB was refreshed. After 48 h, the biofilms were washed once with 100 μL PBS, and 200 μL PDA-NPs (0.5 mg/mL) in PBS were added at 37°C for 20 min and irradiated for 10 min (808 nm, 1300 mW/cm^2). Importantly, TSB is a protein-rich nutrient source for bacteria to grow in, possibly affecting the stability of our PDA-NPs. The observation of heat generation under these conditions negates this assumption.

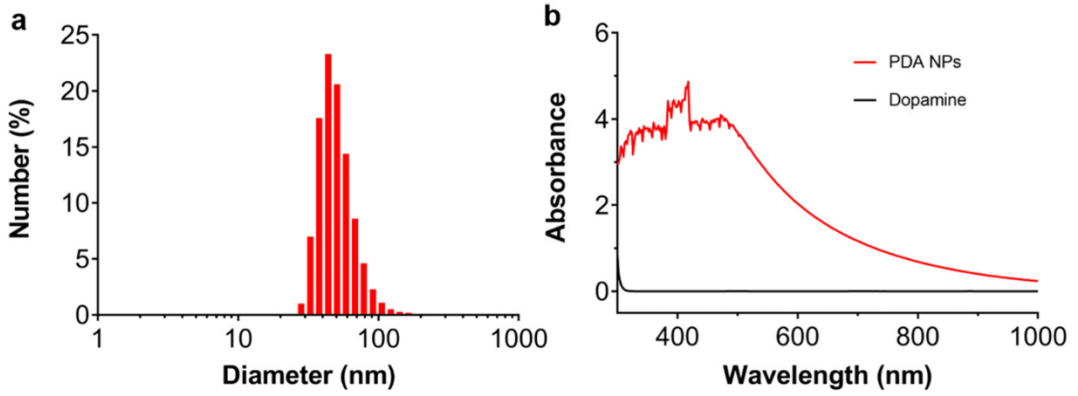

Figure 1. **Characterization and wavelength dependent absorption of polydopamine nanoparticles.**(a) Diameter distribution of PDA-NPs, as measured in water using Dynamic Light Scattering.(b) UV–Vis absorption spectrum of dopamine and PDA-NPs.

For confocal laser scanning microscopy (CLSM), the biofilm was stained with LIVE/DEAD BacLight (3 μL STYO9 and 3 μL propidium iodine in 1 mL demineralized water) at room temperature for 30 min in the dark. After staining, the samples were transferred from 96 well- to 12 well-plates and PBS was added for observation by CLSM. CLSM images were taken using a Leica microscope (LEICA TCS SP2 Leica, Wetzlar, Germany) and 3D reconstructions were created using IMAGE J software (version 1.50b).

A series of similar experiments were carried out, but instead of evaluating the percentage of live/dead staphylococci using staining, biofilm was removed from the glass surfaces by pipetting and sonication for 30 s on ice (30 W) and bacteria suspended in 2.5 mL of PBS. Staphylococcal suspensions were serially diluted and plated on TSB agar plates. After overnight incubation at 37°C, the numbers of CFU were counted. All experiments were carried out with biofilms grown from three separate bacterial cultures.

Photothermal prevention of S. aureus biofilm formation by PDA-NPs

Prophylactic use of photothermal nanoparticles implies the prevention of infectious biofilm formation, as currently achieved e.g. by post-operative administration of antibiotics to prevent the growth of per-operatively introduced bacteria into an infectious biofilm. In analogy with this prophylactic use of antibiotics, staphylococcal biofilms were grown as described above, but in the presence of PDA-NPs. PDA-NPs (0.5 mg/mL) were suspended in the growth medium for the first 24 h or entire growth period of 48 h. After 24 h, the growth medium was refreshed (with or without PDA-NPs), and the biofilm was grown for another 24 h. Control 48 h staphylococcal biofilms were grown in absence of PDA-NPs. All biofilms were irradiated by a NIR-laser (10 min, 808 nm,1300 mW/cm^2). All experiments were carried out with biofilms grown from three separate bacterial cultures.

Tissue cell compatibility

Tissue cell compatibility was evaluated towards L929 fibroblasts using the Cell Counting Kit-8 (CCK-8) assay. Fibroblasts were obtained from the American Type Culture Collection (ATCC-CRL-2014, Manassas, USA) and grown in 75 cm^2 tissue culture polystyrene flasks in RPMI-1640 medium (ThermoFisher Scientific, Inc., Carlsbad, CA) supplemented with 10% Fetal Bovine Serum (FBS, Gibco), 100 U/mL penicillin (Genview) and 100 μg/mL streptomycin (Solarbio) at 37°C in 5% CO_2. Culture media were changed every two days. Cells were grown to 70-80% confluence and detached from the cell-culture flask by trypsinization, collected by centrifugation at 1200 rpm for 5 min and re-suspended in fresh medium to a concentration of 4×10^4 cells/mL, as determined using a Bürker-Türk counting chamber. Then 200 μL cell suspension was placed in 96 well-plates and left to incubate in a humidified 5% CO_2, atmosphere at 37°C for 12 h, after which growth medium was replaced by 200 μL fresh RPMI-1640 medium, supplemented with different concentrations of PDA-NPs, yielding nanoparticle concentrations up to 1 mg/mL. Importantly, suspension of PDA-NPs in this nutrient-rich source supplemented with serum proteins did not affect heat generation or cause visual disassembly of the nanoparticles. After another 24 h of incubation, the medium was removed, and cells washed with PBS for 3 times and CCK-8 solution (20 μL) diluted 1:10 with FBS-free RPMI-1640 (200 μL) was added to each well at 37°C for 1.5 h. Absorbance at 450 nm was subsequently measured using a microplate reader (Thermo, Varioskan Flash) and tissue cell compatibility was expressed as

$$\text{Cell viability}(\%) = \frac{A_{\text{experiment}} - A_{\text{blank}}}{A_{\text{control}} - A_{\text{blank}}} \times 100\% \quad (9)$$

where $A_{experiment}$ and A_{control} are the absorbances of a cell suspension with and without being exposed to PDA-NPs, respectively and A_{blank} is the absorbance of a solution containing FBS-free RPMI-1640 medium and CCK-8 solution, is the mean absorbance of control which contain cells. Each concentration of nanoparticles was evaluated in six-fold using cells from one culture.

Statistical analysis

One-way ANOVA statistical analyses were performed using the Bonferroni multiple comparison correction (GraphPad Prism

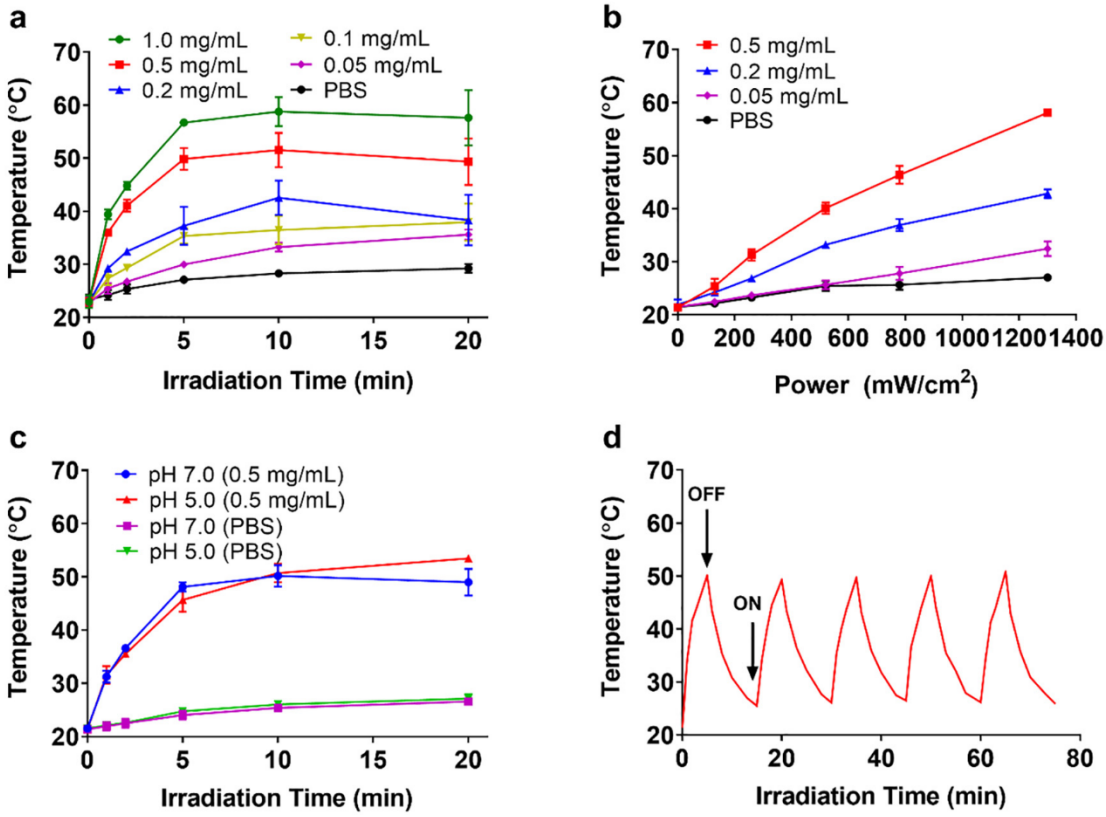

Figure 2. **Photothermal properties of polydopamine nanoparticles suspended in 250 μL PBS upon NIR-irradiation at 808 nm.**(a) Temperature of nanoparticle suspensions at different PDA-NP concentrations as a function of irradiation time (1300 mW/cm^2).(b) Temperature of nanoparticle suspensions at different PDA-NPs concentrations as a function of laser power (irradiation time 20 min).(c) Temperature of PDA-NP suspensions (0.5 mg/mL) and PBS (no nanoparticles) as a function of irradiation time (laser power 1300 mW/cm^2) at pH 5.0 and 7.0.(d) Temperature of PDA-NPs suspensions at different PDA-NPs concentrations as a function of switching the NIR-laser on and off (1300 mW/cm^2). ON/OFF refers to the action of turning the NIR-laser on or off.Error bars represent standard deviations over triplicate measurements with separately prepared batches of nanoparticles.

v. 8.1.1) with statistical significance accepted at $P < 0.05$ for comparing different groups with respect to planktonic bacterial killing and biofilm thickness. Bacterial killing data were log-transformed before performing the ANOVA analyses. Biofilm killing in different groups was compared using a one-way ANOVA with Bonferroni multiple comparison correction, selected for all comparisons changing a single variable (15 comparisons).

Results

PDA-NP characterization and photo-thermal conversion efficiency

The PDA-NPs synthesized had an average hydrodynamic diameter of 85 nm (Figure 1, *a*) and were fully tissue cell compatible (Figure S1). UV-Vis absorption spectroscopy indicated strong absorption of NIR wavelengths by PDA-NPs as compared with dopamine (Figure 1, *b*), confirming their photothermal potential. The $A_{808\ nm}$ required in Eq. 6 to calculate the photothermal conversion efficiency was taken from Figure1, *B* to equal 0.66.

Figure 2 presents the necessary temperature data to calculate the photothermal conversion efficacy of the PDA-NPs synthesized. Higher concentrations of PDA-NPs yielded higher system temperatures, reaching equilibrium within 10 min (Figure 2, *A*). For a PDA-NP concentration of 0.5 mg/mL and an NIR-irradiation of 0.5 W, it can be read that $\Delta T_{max,\ suspension}$ as occurring in Eq. 6 amounts 28.5°C. System temperatures also increased with increasing irradiation power (Figure 2, *B*), while the suspension pH (7.0 under physiological conditions[40] and around 5.0 in a biofilm[45]) had no influence upon the photothermal efficiency of the nanoparticles (Figure 2, *C*). Note that also NIR-irradiation of the system in absence on PDA-NPs yielded a minor increase in temperature (see also Figure 2, *A*), reaching a maximum equilibrium temperature $\Delta T_{max,\ H_2O}$ as occurring in Eq. 6 after NIR-irradiation at 0.5 W, that amounted 4.9°C. Heat losses of the system were evaluated by switching the NIR-laser on and off, while monitoring temperature increases and decreases, respectively (Figure 2, *D*). Presentation of the logarithm of temperature decrease as a function of time yielded a linear relation (Figure S2), according to Eq. 8. Using the mass (0.25×10^{-3} kg) and the specific heat (4.2×10^3J kg^{-1} °C^{-1}) of water, hA follows from the slope and Eq. 8 (0.0034 J/(s cm^2)) and the photothermal conversion efficiency η of our PDA-NPs

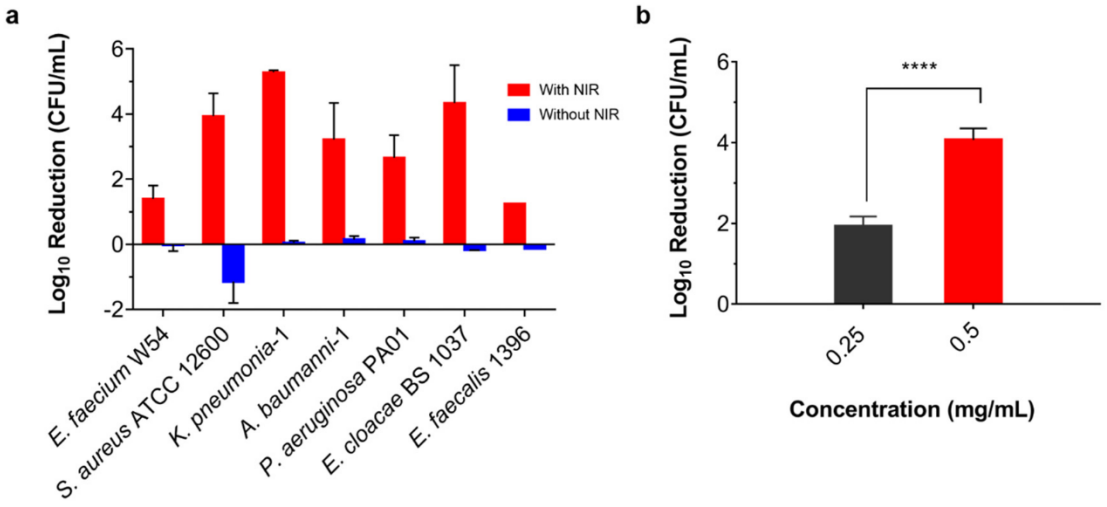

Figure 3. **Killing of planktonic ESKAPE-panel pathogens (3×10^6 CFU/mL) in 250 µL suspensions with polydopamine nanoparticles upon NIR-irradiation (808 nm for 10 min at 1300 mW/cm^2).**(a) Log-reduction in CFUs of planktonic ESKAPE-panel members in the presence of 0.5 mg/mL PDA-NPs upon NIR-irradiation (*E. faecalis* could only be evaluated in single-fold).(b) Log-reduction in CFUs of planktonic *S. aureus* ATCC 12600 in the presence of different concentrations of PDA-NPs upon NIR-irradiation.Log_{10} CFUs of ESKAPE-panel pathogens in absence of PDA-NPs and NIR-irradiation amounted 6.2 on average. Error bars represent standard deviations over triplicate experiments. ****Statistical significance at $P < 0.0001$ (one-way ANOVA, Bonferroni).

synthesized can be calculated to be 21%. This is lower than the conversion efficiency of core–shell nano-plates of Pd and Au (29%),[46] but similar to gold nano-rods (22%) and higher than of gold nano-shells (13%).[47]

Killing of planktonic ESKAPE-panel pathogens by photo-activated polydopamine nanoparticles

Bacterial killing efficacy of PDA-NPs was evaluated against ESKAPE-panel pathogens in suspension (3×10^6 CFU/mL), including *E. faecium* W54, *S. aureus* ATCC 12600, *K. pneumonia*-1, *A. baumanni*-1, *P. aeruginosa* PA01, and *Enterobacter cloacae* BS 1037 and additionally *Enterococcus faecalis* 1396 (NIR-irradiation at 808 nm and 1300 mW/cm^2 for 10 min). NIR-irradiation at a PDA-NP concentration of 0.5 mg/mL in the volume employed (250 µl) yielded a temperature increase to 50.1°C (Figure 2, *A*). Neither the presence of PDA-NPs in absence of NIR-irradiation nor NIR-irradiation in absence of PDA-NPs yielded killing of ESKAPE member pathogens in relevant numbers (< 0.2 log-unit reductions). However, NIR-irradiation of suspensions with PDA-NPs and ESKAPE-panel members caused three to five log-unit reductions, with the exception of *Enterococcus* spp. (Figure 3, *A*). For *E. faecium* and *E. faecalis* species, photothermal killing was limited to maximally two-log unit reductions. Photothermal killing was significantly less at a lower nanoparticle to bacteria ratio, as illustrated in Figure 3, *B* for *S. aureus* ATCC 12600.

Photothermal effects on existing staphylococcal biofilms exposed to PDA-NPs in suspension

Eradication of an existing 48 h *S. aureus* ATCC 12600 biofilm on glass surfaces was evaluated by exposing biofilms to a suspension of PDA-NPs (0.5 mg/mL in a volume of 200 µL) with and without 10 min NIR-irradiation at 808 nm (1300 mW/cm^2). Growth of biofilms on a glass sample added a second heat-absorbing component, i.e. the glass sample, to the system, but its heat capacity (0.04 J/°C) is negligible compared to the heat capacity of the water (1.05 J/°C) and it can be assumed that the same maximal temperature can be reached as in absence of the glass sample (50.1°C; see Figure 2, *A*). LIVE/DEAD staining of the biofilms grown followed by CLSM imaging (Figure 4), showed that the biofilms had an average thickness of 36 ± 7 µm, corresponding well with clinical thicknesses of biofilm infections.[24] *S. aureus* biofilm thickness was neither affected by NIR-irradiation in the absence of PDA-NPs nor in presence of PDA-NPs in suspension above the biofilm.

Regardless of the absence or presence of PDA-NPs or their NIR-irradiation, staphylococcal biofilms were predominantly green-fluorescent, indicative of live bacteria, with very little dead, red-fluorescent bacteria (see also Figure 4). Note that although live/dead staining is generally applied to demonstrate bacterial cell death, it technically only implies cell wall damage.[48] Therefore, conclusions derived from live/dead staining were verified by CFU enumeration. Removal of biofilms and subsequent CFU enumeration, only indicated slightly lower numbers of CFUs in presence of PDA-NPs before and after NIR-irradiation (Figure 5). This supports our conclusions drawn from live/dead staining.

Photothermal effects on staphylococcal biofilm formation grown in the presence of PDA-NPs

Prophylactic use of antimicrobials implies preventing growth of a bacterial biofilm while being exposed to antimicrobials. Therefore, in order to mimic prophylactic conditions, staphylococcal biofilms were grown in the presence of PDA-NPs in the growth medium during the initial 24 h of growth (Figure 6) or during the entire 48 h period of growth (Figure S3), with or without NIR-irradiation. NIR-irradiation in absence of PDA-NPs during growth did not affect the number of green-fluorescently

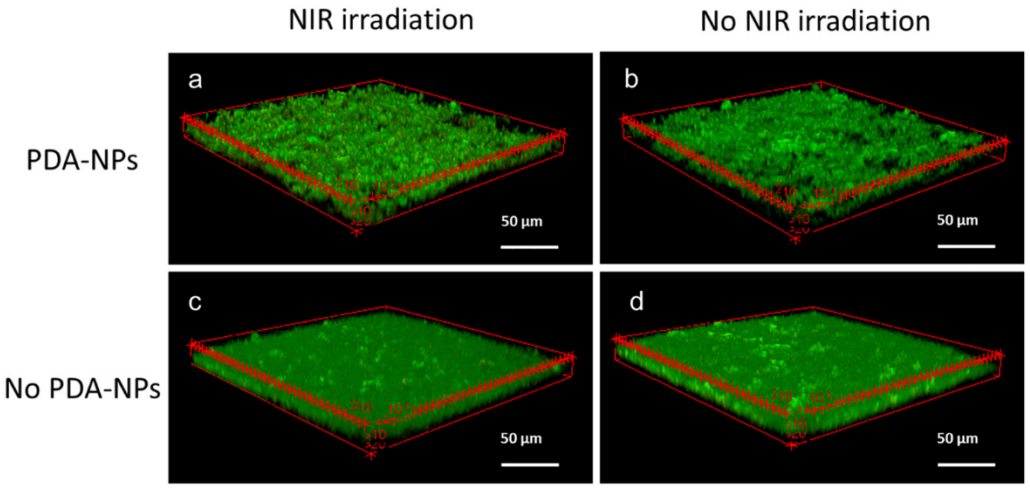

Figure 4. **Photothermal effects on existing 48 h old, *S. aureus* ATCC 12600 biofilms in the absence or presence of PDA-NPs (0.5 mg/mL) in suspension (200 µL) above the biofilms and with and without NIR-irradiation (10 min NIR-irradiation at 1300 mW/cm^2). Total exposure time to a PDA-NP suspension was 20 min. After photothermal treatment, biofilms were Live/Dead stained for CLSM imaging.**(a) CLSM image of staphylococcal biofilm in the presence of PDA-NPs in suspension above the biofilms after NIR-irradiation.(b) A staphylococcal biofilm in the presence of PDA-NPs in suspension above the biofilms without NIR-irradiation.(c) A staphylococcal biofilm in the absence of PDA-NPs in suspension above the biofilms after NIR-irradiation.(d) A staphylococcal biofilm in the absence of PDA-NPs in suspension above the biofilms without NIR-irradiation.

stained staphylococci (Figures 6, *C* and *D* and Figures S3, *C* and *D*). Growth in the presence of PDA-NPs yielded red-fluorescent staphylococci also in absence of NIR-irradiation (Figures 6, *B* and S3, *B*). Verification of staphylococcal killing by PDA-NPs in absence of NIR-irradiation using agar-plating did not yield any reduction in CFUs (Figure 5), supporting again the conclusions from live/dead staining and indicative of bacterial survival despite the cell wall damage done by PDA-NPs. NIR-irradiation and subsequent heat dissipation by PDA-NPs incorporated during growth in the biofilm yielded red-fluorescence (i.e. membrane damage) in nearly all staphylococci (Figures 6, *A* and S3, *A*), accompanied by a reduced number of CFUs (Figure 5). CFU reduction was larger when biofilms were grown in the presence of PDA-NPs during the entire 48 h of growth than when solely present during the initial 24 h of growth.

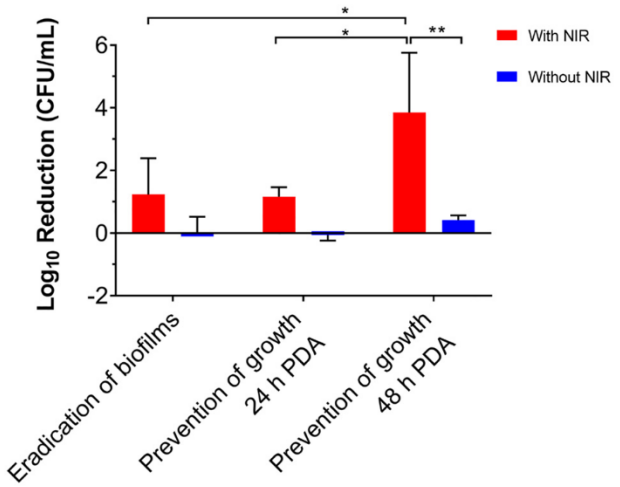

Figure 5. **Photothermal killing of 48 h *S. aureus* ATCC 12600 biofilms after NIR-irradiation of biofilms exposed to PDA-NPs in suspension (compare Figure 4) and during growth in the presence of PDA-NPs during the initial 24 h of growth or during the entire 48 h period of growth (Figures 6 and S3).** NIR-irradiation was always done after 48 h of growth. Error bars represent standard deviations over triplicate experiments with different bacterial cultures. Significance was tested using a one-way ANOVA test with Bonferroni correction, * $P < 0.05$, ** $P < 0.01$).

Discussion

PDA-NPs were prepared with a photothermal conversion efficiency of 21% without further surface modification. Various types of surfaces modification have been applied to PDA-NPs (see also the Background section to this article), to allow blood circulation, targeting biofilm penetration and enhance bacterial killing.[49,50] Surface modifications can be applied to PDA-NPs through Michael addition or Schiff base reactions[35,51] but frequently yields loss of biocompatibility[30,52] therewith making clinical translation more difficult than with unmodified PDA-NPs possessing proven biocompatibility (Figure S1).[53] Unfortunately, nanoparticle to bacteria ratios, but also suspension volumes and laser power densities vary across the literature, which makes comparison of our results with other studies difficult. Within the limitations of current literature description in which these essential features for adequate comparison with other studies are often missing, our unmodified PDA-NPs probably have a higher photothermal conversion efficacy and better cell tissue compatibility than surface modified PDA-NPs. In addition, unmodified PDA-NPs can be bio-degraded to pyrrole-2, 3-dicarboxylic acid, and pyrrole-2,3-dicarboxylic acid by hydrogen peroxide as widely distributed in phagocytes and various organs.[32,36]

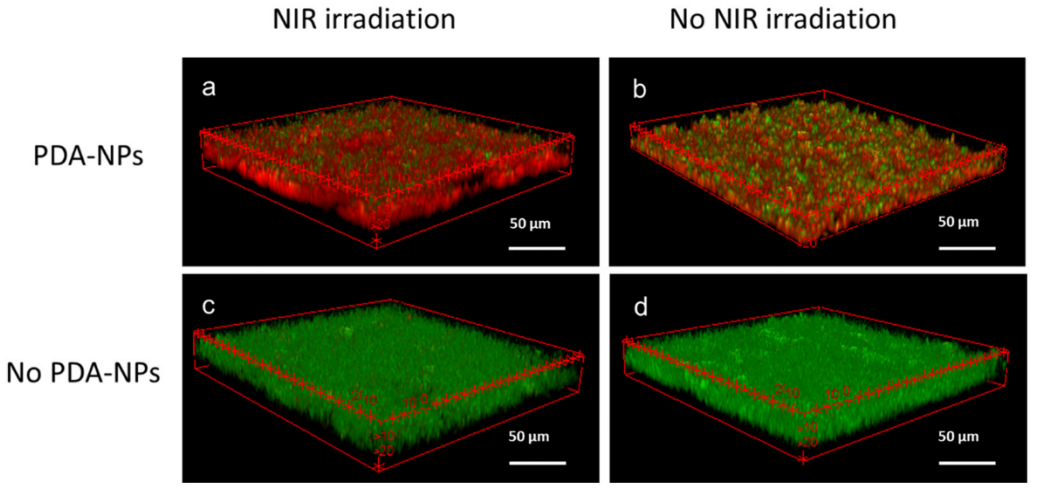

Figure 6. **Photothermal effects on *S. aureus* ATCC 12600 biofilms formation during 48 h of growth in the absence or 24 h initial presence of PDA-NPs in 200 µL growth medium (0.5 mg/mL) and with and without NIR-irradiation.** CLSM images of the staphylococcal biofilms were taken after 48 h, before and after 10 min NIR-irradiation at 1300 mW/cm^2. After photothermal treatment, biofilms were Live/Dead stained for CLSM imaging.(a) CLSM image of staphylococcal biofilm grown in presence of PDA-NPs after NIR-irradiation.(b) A staphylococcal biofilm grown in the presence of PDA-NPs without NIR-irradiation.(c) A staphylococcal biofilm grown in the absence of PDA-NPs after NIR-irradiation.(d) A staphylococcal biofilm grown in the absence of PDA-NPs without NIR-irradiation.

Most of our evaluation experiments were done in volumes between 200 - 250 µL at a PDA-NP concentration of 0.5 mg/mL and 808 nm NIR-irradiation (1300 mW/cm^2) for 10 min, yielding a temperature increase to approximately 50°C (Figure 2, *A*). This is at the higher end of the therapeutic temperature range that does not produce collateral tissue damage.[15] For *E. faecium* and *E. faecalis* species, photothermal killing under these conditions was limited to maximally two-log unit reductions (Figure 3, *A*). Since two-log unit reductions are microbiologically and clinically meaningless, these strains may be classified as thermo-resistant human pathogens. This points to the potential danger of thermo-resistance in infectious pathogens if photothermal treatment of infections becomes large-scale used in the clinic. After all, thermo-resistant bacteria exist in natural environments[54] and industrial applications.[55] Horizontal gene-transfer[56] in infectious biofilms between more and less thermo-resistant inhabitants can easily convey thermo-resistance to an entire population, as common in the spreading of antibiotic resistance.[57] For other ESKAPE panel pathogens, three to five log-unit reductions were observed that may seem large, but photothermal killing of planktonic bacteria must always be judged in relation with the ratio at which photothermal nanoparticles and target bacteria are suspended, as illustrated for photothermal *S. aureus* killing (Figure 3, *B*). Overall however, other photothermal nanoparticles described in the literature showed less than two log-unit reduction in CFU upon NIR-irradiation.[38] This suggests, that PDA-NPs in absence of surface-modification are highly effective in photothermal killing of a wide variety of bacterial strains and species.

This article shows that there is no therapeutic effect to be expected from photothermal treatment with PDA-NPs when applied to an existing biofilm, neither based on live-dead staining (Figure 4) nor on the basis of CFU enumeration (Figure 5). Conclusions on bacterial killing from live/dead were supported here by CFU enumeration which is important, because technically, live-dead staining only implies cell wall damage[48] that can sometimes be self-repaired without impeding bacterial growth and colony formation on agar plates,[58,59] which still is the gold standard for bacterial death in clinical microbiology.[60,61] Absence of therapeutic effects can be explained by lack of penetration of unmodified photothermal nanoparticles in the biofilms, causing heat dissipation in the aqueous surrounding of the biofilm rather than inside it.

Opposite to therapeutic benefits, prophylactic benefits of unmodified PDA-NP were demonstrated in our article (Figures 5, 6 and S3). Prophylactic benefits imply that photothermal treatment commences before or during the onset of biofilm growth, similar to the prophylactic use of antibiotics. PDA-NPS incorporated in a biofilm during its growth demonstrated minor bacterial killing ability even in absence of NIR-irradiation. This is in line with other studies, showing minor killing of bacteria adhering on polydopamine layers adsorbed to different substrata.[62,63] Antibacterial efficacy of PDA-NPs in absence of NR-irradiation was not observed in planktonic evaluation (Figure 3) and existing biofilm eradication (Figure 4), probably because intimate contact between polydopamine and bacterial cell surfaces is needed that only occurs during growth of bacteria in presence of PDA-NPs. Bacterial growth in the presence of PDA-NPs was much more strongly reduced upon NIR-irradiation than in its absence. This suggests potential of unmodified PDA-NPs for infection prophylaxis, as after invasive surgery or trauma.

Exposure to PDA-NPs and subsequent NIR-irradiation of ESKAPE-panel pathogens demonstrated that particularly enterococci were more heat-resistant than other members of the ESKAPE-panel, most notably *S. aureus*. This constitutes a warning that development of thermo-resistance in human infectious pathogens may not *a priori* be excluded and warrants

more research in the development of thermo-resistance by human pathogens if photothermal infection-control is going to be large-scale clinically applied.

PDA-NPs in suspension above an existing biofilm did not cause significant killing of bacteria in the biofilm. This implies that clinically, photothermal nanoparticles without surface modification to enhance biofilm penetration have no therapeutic potential. This is different for their prophylactic potential: biofilm growth in the presence of photothermal nanoparticles and after NIR-irradiation, killed significant numbers of bacteria during biofilm formation. Currently, antibiotics are applied prophylactically to prevent infectious biofilm formation in the immediate period after invasive surgery or trauma. This type of prophylactic antibiotic administration is either orally or by local administration at a surgical-site, from which the antibiotics gradual diffuse away to become cleared from the body, enabling clinically-desired, short term antibiotic protection and infection prevention. Usually, broad spectrum antibiotics are given for these purposes which can cause collateral damage to the healthy microflora in the human body. Local administration at the surgical-site of highly biocompatible, unmodified photothermal nanoparticles and their temporary presence due to clearance from the body, would also be ideal to prevent surgical-site infection in the immediate period post-surgery. Photodynamic therapy avoids collateral damage to the healthy microflora as NIR-irradiation can be confined to the infection site.

Herewith, we have cleared a pathway for the clinical translation of unmodified photothermal PDA-NPs, identifying limitations and opportunities.

CRediT author statement

RG: Investigation, Formal Analysis, Methodology, Writing (First draft and editing); **HCvdM:** Project Supervision, Resources, Methodology, Writing (editing), Project Administration; **YR:** Project Administration, Writing (editing); **HC:** Project Administration, Funding Acquisition, Writing (editing); **GC:** Project Administration, Funding Acquisition, Writing (editing); **HJB:** Conceptualization, Project Supervision, Methodology, Visualization, Writing (editing), Funding Acquisition; **BWP:** Investigation, Formal Analysis, Methodology, Project Supervision, Writing (editing)

Appendix A. Supplementary data

Supplementary data to this article can be found online at https://doi.org/10.1016/j.nano.2020.102324.

References

1. Zhao G, Usui ML, Lippman SI, James GA, Stewart PS, Fleckman P, et al. *Adv Wound Care* 2013;**2**:389-99.
2. Bassetti M, Poulakou G, Ruppe E, Bouza E, Van Hal SJ, Brink A. *Intensive Care Med* 2017;**43**:1464-75.
3. Conlon BP, Nakayasu ES, Fleck LE, LaFleur MD, Isabella VM, Coleman K, et al. *Nature* 2013;**503**:365-70.
4. Gupta P, Sarkar S, Das B, Bhattacharjee S, Tribedi P. *Arch Microbiol* 2016;**198**:1-15.
5. Durmus NG, Taylor EN, Kummer KM, Webster TJ. *Adv Mater* 2013;**25**:5706-13.
6. Chenthamara D, Subramaniam S, Ramarishnan SG, Krishnaswamy S, Essa MM, Lin F-H, et al. *Biomater Res* 2019;**23**20, https://doi.org/10.1186/s40824-019-0166-x.
7. Cheow WS, Chang MW, Hadinoto K. *Colloids Surf A Physicochem Eng Asp* 2011;**389**:158-65.
8. Ratto F, Matteini P, Centi S, Rossi F, Pini R. *J Biophotonics* 2011;**4**:64-73.
9. Markovic ZM, Harhaji-Trajkovic LM, Todorovic-Markovic BM, Kepic DP, Arsikin KM, Jovanovic SP, et al. *Biomaterials* 2011;**32**:1121-9.
10. Gao S, Zhang L, Wang G, Yang K, Chen M, Tian R, et al. *Biomaterials* 2016;**79**:36-45.
11. Zhu Z, Su M. *Nanomaterials* 2017;**7**:160, https://doi.org/10.3390/nano7070160.
12. Zha Z, Yue X, Ren Q, Dai Z. *Adv Mater* 2013;**25**:777-82.
13. Meng Y, Wang S, Li C, Qian M, Yan X, Yao S, et al. *Biomaterials* 2016;**100**:134-42.
14. Liang Y, Zhao X, Hu T, Chen B, Yin Z, Ma PX, et al. *Small* 2019;**15**e1900046.
15. Jaque D, Martinez Maestro L, del Rosal B, Haro-Gonzalez P, Benayas A, Plaza JL, et al. *Nanoscale* 2014;**6**:9494-530.
16. Meeker DG, Jenkins SV, Miller EK, Beenken KE, Loughran AJ, Powless A, et al. *ACS Infect Dis* 2016;**2**:241-50.
17. Mocan L, Matea C, Tabaran FA, Mosteanu O, Pop T, Puia C, et al. *Sci Rep* 2016;**6**:39466.
18. Dai X, Zhao Y, Yu Y, Chen X, Wei X, Zhang X, et al. *Nanoscale* 2018;**10**:18520.
19. Xu J-W, Yao K, Xu Z-K. *Nanoscale* 2019;**11**:8680.
20. Nam J, Son S, Ochyl LJ, Kuai U, Schwendeman A, Moon JJ. *Nat Commun* 2018;**9**1074.
21. Pereyra JY, Cuello EA, Sallavagione HJ, Barbero CA, Acevedo DF, Yslas EI. *Photodiagn Photodyn Ther* 2018;**24**:36-43.
22. Zhu C, Shen H, Liu H, Lv X, Li Z, Yuan Q. *Chem Eur J* 2018;**24**:19060-5.
23. Jin Y, Deng J, Yu J, Yang C, Tong M, Hou Y. *J Mater Chem B* 2015;**3**:3993.
24. Hoiby N, Bjarnsholt T, Givskov M, Molin S, Ciofu O. *Int J Antimicrob Agents* 2010;**35**:322-32.
25. Del Pozo JL, Anti Expert Rev. *Infect Ther* 2018;**16**:51-65.
26. Pallavicini P, Dona A, Taglietti A, Minzioni P, Patrini M, Dacarro G, et al. *Chem Commun* 2014;**50**:1969.
27. Park D, Kim J, Lee YM, Park J, Kim WJ. *Adv Heatlhcare Mater* 2016;**5**:2019-24.
28. Yang C, Ding X, Ono RJ, Lee H, Hsu LY, Tong YW, et al. *Adv Mater* 2014;**26**:7346-51.
29. Ding X, Yang C, Lim TP, Hsu LY, Engler AC, Hedrick JL, et al. *Biomaterials* 2012;**33**:6593-603.
30. Li Y, Jiang C, Zhang D, Wang Y, Ren X, Ai K, et al. *Acta Biomater* 2017;**47**:124-34.
31. Dong Z, Gong H, Gao M, Zhu W, Sun X, Feng L, et al. *Theranostics* 2016;**6**:1031.
32. Liu Y, Ai K, Liu J, Deng M, He Y, Lu L. *Adv Mater* 2013;**25**:1353-9.
33. Hong S, Kim KY, Wook HJ, Park SY, Lee KD, Lee DY, et al. *Nanomedicine* 2011;**6**:793-801.
34. Han J, Park W, Park SJ, Na K. *ACS Appl Mater Interfaces* 2016;**8**:7739-47.
35. Liu Y, Ai K, Lu L. *Chem Rev* 2014;**114**:5057-115.
36. Bettinger CJ, Bruggeman JP, Misra A, Borenstein JT, Langer R. *Biomaterials* 2009;**30**:3050-7.
37. Yuan Z, Tao B, He Y, Mu C, Liu G, Zhang J, et al. *Biomaterials* 2019;**223**:119479.
38. Hu D, Zou L, Li B, Hu M, Ye W, Ji J. ACS Biomater. *Sci Eng* 2019;**5**:5169-79.

39. Ye Q, Zhao J, Wan Q, Qiao B, Zhou J. *Transpl Infect Dis* 2014;**16**:767-74.
40. Kramer ML, Kratzin HD, Schmidt B, Romer A, Windl O, Liemann S, et al. *J Biol Chem* 2001;**276**:16711-9.
41. Santajit S, Indrawattana N. *Biomed Res Int* 2016;**2016**:2475067.
42. Pendleton JN, Gorman SP, Gilmore BF. *Expert Rev Anti-Infect Ther* 2013;**11**:297-308.
43. Reddy PN, Srirama K, Dirisala VR. *Infect Dis* 2017:10, https://doi.org/10.1177/1179916117703999.
44. Ren W, Yan Y, Zeng L, Shi Z, Gong A, Schaaf P, et al. *Adv Healthcare Mater* 2015;**4**:1526-36.
45. Percival SL, McCarty S, Hunt JA, Woods EJ. *Wound Rep Reg* 2014;**22**:174-86.
46. Chen M, Tang S, Guo Z, Wang X, Mo S, Huang X, et al. *Adv Mater* 2014;**26**:8210-6.
47. Huang P, Lin J, Li W, Rong P, Wang Z, Wang S, et al. *Angew Chem Int Ed* 2013;**52**:13958-64.
48. Boulos L, Prevost M, Barbeau B, Coallier J, Desjardins R. *J Microbiol Methods* 1999;**37**:77-86.
49. Forier K, Messiaen AS, Raemdonck K, Nelis H, De Smedt S, Demeester J, et al. *J Controlled Rel* 2014;**195**:21-8.
50. Ikuma K, Decho AW, Lau BL. *Front Microbiol* 2015;**6**:591.
51. Yang H-C, Waldman RZ, Wu M-B, Hou J, Chen L, Darling SB, et al. *Adv Funct Mater* 2018;**1705327**:28.
52. Ho C-C, Ding S-J. *J Mater Sci Mater Med* 2013;**24**:2381-90.
53. Singh I, Priyam A, Jha D, Dhawan G, Gautam HK, Kumar P. *Mater Sci Eng C* 2020;**110284**:107.
54. Sen SK, Mohapatra SK, Satpathy S, Rao GT. *Int J Chem Res, ISSN* 2010;**0975-3699**(2):01-7.
55. Gleeson D, O'Connell A, Jordan K. *Ir J Agric Food Res* 2013;**52**:217-27.
56. Nesse LL, Simm R. *Adv Appl Microbiol* 2018;**103**:223-46.
57. Vatansever F, de Melo WC, Avci P, Vecchio D, Sadasivam M, Gupta A, et al. *FEMS Microbiol Rev* 2013;**37**:955-89.
58. Berney M, Hammes F, Bosshard F, Weilenmann HU, Egli T. *Appl Environ Microbiol* 2007;**73**:3283-90.
59. Joux F, Lebaron P. *Microbes Infect* 2000;**2**:1523-35.
60. Sachidanandham R, Gin KY, Poh CL. *Biotechnol Bioeng* 2005;**89**:24-31.
61. Rosen DK, Gallardo M, Vail M, Hellberg RS, Microbiol J. *Methods* 2020, https://doi.org/10.1016/j.mimet.2020.105881.
62. Fan Y-J, Pham MT, Huang C-J. *Langmuir* 2018;**35**:1642-51.
63. Su L, Yu Y, Zhao Y, Liang F, Zhang X. *Sci Rep* 2016;**6**:24420.